Development of Simple Radar Signature Models for Knowledge-Aided Wind Turbine Radar Interference Analysis

Ying Bai[1, 2] , Yan Zhang[1, 2], Fanxing Kong[1,2] , and Robert Palmer[1,3]
1: Atmospheric Radar Research Center (ARRC), University of Oklahoma
2: School of Electrical and Computer Engineering, University of Oklahoma
3: School of Meteorology, University of Oklahoma
ying.bai@ou.edu, rockee@ou.edu, fxkong@ou.edu, and rpalmer@ou.edu

Abstract

Wind power technology has been well-established for many years and the benefits are widely known in terms of the importance of renewable energy source. Wind farm installations close to weather radars may block the normal propagation of the radar signals and cause severe interference. In order to mitigate the contamination of wind turbine clutter (WTC) in radar sensors with tractable computational load, it is very important to understand the radar signature of WTC and be able to generate a simple signal model to capture its features.

In this work, characteristics of the scaled wind turbine model are analyzed both in lab measurement and EM simulation. It is easy to set various kinds of conditions with EM solvers. However, it imposes a prohibitive computational burden on large size models. Thus, a simplified mathematical model is created to captures the features of radar backscattering signatures from WTC. The wave scattering from a rotating target is modulated in amplitude and phase. As such, both the amplitude and phase signatures of this simplified model are calculated and compared with EM simulation.

1. INTRODUCTION

1.1. Trend of Wind Energy

The utilization of wind turbines has been a great way to harness the energy of the wind in a bid to convert this into useable electricity. Harness the winds energy with a wind turbine can provide a source of clean and renewable electricity for large or small communities. Some wind farms are capable of providing the entire electricity supply for large villages or small towns. Wind turbines are found in a variety of countries across the globe and have a key presence in areas such as American and Europe. Currently, wind farm installations can have over a hundred turbines of up to 120m height each. Moreover, turbines are expected to be larger in size in a few years, with blade tip heights reaching 200m.

1.2. Impact of Wind Farms on Radar Observations

Wind turbines can cause interference to radars, especially when grouped into large wind farms, either by creating unwanted reflections or by blocking signals which can result in clutter on radar displays. The tremendous obstacles caused by wind farm on the radar screen will cause the potentially devastating storm and other weather detection and alarm having become more complex.

As a case study about WTC affecting on weather radar's Level-II data, the two images in Fig. 1 are from two different dates, August 4, 2005 on the left and June 19, 2005 on the right. The right figure is in a clear air. Wind farms are located in the red circle, and can be clearly observed by the radar. Unfortunately, it is hard to distinguish between storm and WTC in severe weather condition for left figure [1].

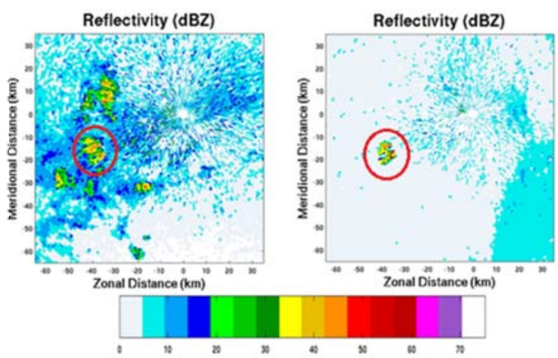

Figure 1: Level-II PPI plots of radar reflectivity from KDDC. The left figure is taken on August 4, 2005 and the right one is on June 19, 2005.

2. WTC CHARACTERIZATION

In this research, two methods are used to identify wind turbines' characterizations and to compare the signatures.

2.1. Lab Measurement

A scaled wind turbine model with blade length of 0.3m was customized to emulate a real wind turbine. A rotor is installed to control blade rotation; and the model is placed on a rotary stage to control the yaw angle, which is the angle between the rotor axis of turbine and the radar LOS. In addition, a scatterometer is designed to emulate the real radar. All equipment is located in an anechoic chamber. Fig. 2 depicts the measurement configuration. The distance between the scaled model and antennas is about 3m, which is in the far field.

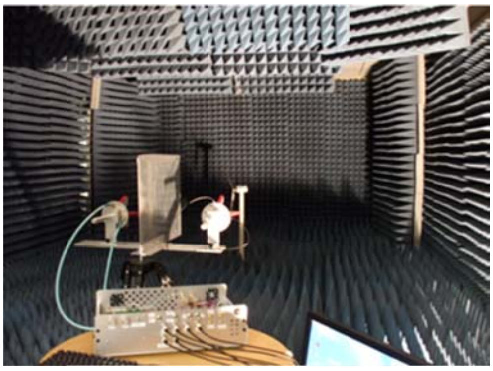

Figure 2: The lab measurement configuration in an anechoic chamber. The scaled model is placed 3m away from antennas.

2.2. EM Simulation

Classic wind turbine structure is consisted of tower, nacelle and rotating blades. Since the stationary clutter, such as tower and nacelle (considering station), can be easily removed by GMAP (Gaussian Model Adaptive Processing) [2]. The rotating blade is the primary concern of this study and there is currently no technique to remove such interference.

A scaled three-blade model is built independently using advanced design tools (i.e. SolidWorks) and is divided into many small triangular flat plates (called facets). Fig. 3 illustrates the geometry of the scaled three-blade model. The scattering from each facet is computed using the Physical Optics approximation technique. Therefore, the total RCS of the object is coherent superposition of the RCSs of all of the facets. In this method, a MATLAB code [3] is adopted to calculate the RCS.

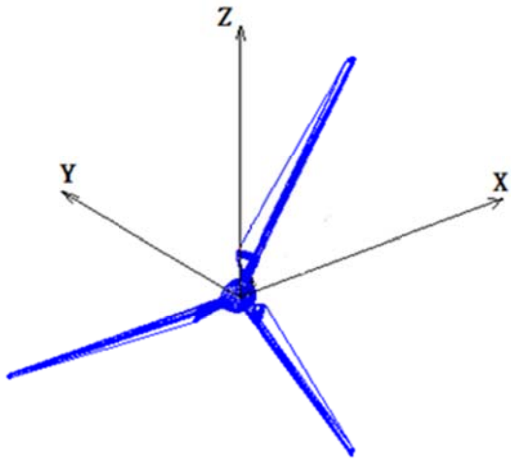

Figure 3: Geometry of a scaled three-blade model in EM simulation. The blade length of turbine is 0.3m. A radar with 10.5GHz carrier frequency is operating at z-axis (90^0 yaw angle), the initial blade position is zero.

EM simulation is a conventional and accurate way to calculate the RCS of a target. However, for different types and orientations of wind turbine structures, they must be remodeled each time; and the computational time is too long for large size models.

2.3. Comparison

Fig. 4 compares the RCS with respect to blade position obtained from lab measurement and EM simulation. Both curves have six major peaks when a blade sweeps an entire cycle (360^o). The three higher peaks occur when one of blade leading edge is perpendicular to radar LOS; while the other three lower peaks occur when one of trailing edge is vertical to the radar. There are several reasons to cause curves' mismatch. In EM simulation, multiple reflections, diffraction and surface waves are not included; and in lab measurement, manual placement of physical model might be imprecise. However, the EM simulation result is able to reasonably match that of the lab measurement.

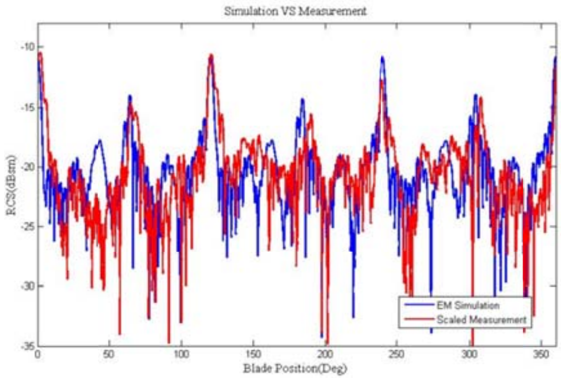

Figure 4: RCS (dBsm) versus blade position (degrees), comparing between lab measurement and EM simulation. One of blades is at upper vertical position, and the radar is observing the structure from 90^o yaw angle.

3. SIMPLFIED RADAR SIGNATURE MODEL

The training data of WTC from field measurements is limited, and it should be combined with a-prior knowledge. On the other hand, clutter signal models based on electromagnetic solvers and analysis are complicated and time-consuming. Therefore, a simplified, maybe statistical signature framework is needed, in order to "fuse" the WTC training data from different sources. When an object is rotating, the radar signature from it is modulated in amplitude and phase. To simply the calculation on wind turbine model, the amplitude and phase information are separately considered in this research.

3.1. Amplitude Model

To capture the amplitude features of the radar backscattering from rotating blades, a simplified model is created, as shown in Fig. 5. Each blade consists of three different shape objects: cylinder, rectangular flat plate and triangular flat plate.

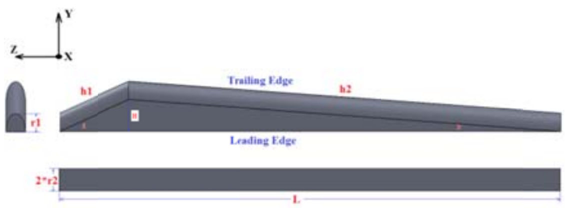

Figure 5: Geometry of a simplified blade model. A blade is composed of three basic shape objects: elliptical cylinder, rectangular plate and triangular plate.

The RCS of this model can be computed by combining the cross section of these three simple objects. The formulations in PO approximation [4] are shown bellowing:

Cylinder:

$$\sigma = \frac{\lambda r_2^2 r_1^2 sin\theta}{8\pi(cos\theta)^2[r_1^2(cos\phi)^2 + r_2^2(sin\phi)^2]^{1.5}} \quad (1)$$

Rectangular Plate:

$$\sigma = \frac{4\pi A^2}{\lambda^2} cos^2\theta sinc^2(2kr_2u)sinc^2(kLv)$$

$$u = sin\theta cos\phi, v = sin\theta sin\phi \quad (2)$$

Triangular Plate:

$$\sigma = \frac{4\pi A^2}{\lambda^2} cos^2\theta[sinc^4\alpha + \frac{(sin2\alpha - 2\alpha)^2}{4\alpha^4}]$$

$$\alpha = kr_1 sin\theta cos\phi, \beta = 2kr_2 sin\theta sin\phi \quad (3)$$

Where λ is wavelength, r_1, r_2 are the radius of the cylinder, A is the area, k is the wave number, θ, ϕ are the direction angle.

3.2. Phase Model

In order to derive a phase model of radar signatures, the geometry of the radar and the rotating blades are displayed in Fig. 6. The radar is located at the origin of the space-fixed coordinates (X, Y, Z) and the rotor blades are centered at the origin of body-fixed coordinates (x, y, z) on the x-z plane rotating clockwise about the y-axis with an angular rotation rate ω. The radar observed azimuth and elevation angle are α and β. The blades are simplified as rectangular plates and are assumed consist of scattering centers with the same reflectivity.

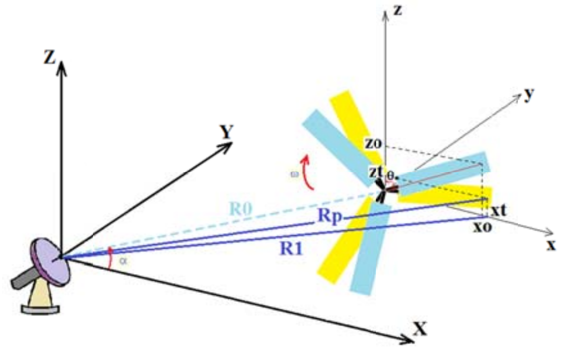

Figure 6: Geometry of the radar and the rotating blades. The blades are rotating clockwise with an angular rotation rate ω. The radar observed azimuth and elevation angle are α and β.

The complex return signal from rotating N-blades [5] is

$$S_{\sum}(t) = Lexp[j(2\pi f_0 t - \frac{4\pi}{\lambda}(R_0 + \frac{L}{2}cos\beta cos\alpha' cos(\frac{\pi}{2} - \theta_0 - \omega t))] \sum_{k=0}^{N-1} sinc(A) \quad (4)$$

Where the phase function is

$$A = \frac{4\pi}{\lambda}\frac{L}{2}cos\beta cos\alpha' cos(\pi/2 - \theta_0 - \omega t + \frac{k2\pi}{N}) \quad (5)$$

Where L is blade length, λ is wavelength, R_0 is the distance from the radar to the origin of turbine, $\alpha' = \alpha + \phi$ is equated azimuth angle, α is azimuth angle, ϕ is turbine rotation angle, θ_0 is initial blade position, ω is angular rotation rate and N is the number of blades. These radar parameters, wind turbine dynamics and observation aspect angle can be known in real measurement.

4. COMPARISION BETWEEN SIMPLE MODEL RESULT AND EM SIMULATION OUTPUT

This section details the result from simplified model and compares it with EM simulation in terms of amplitude, phase and Micro-Doppler spectrum. A similar scenario is assumed: radar is operating at 90^o yaw angle with 10.5GHz and the initial blade position is one of blade leading edge is at upper vertical.

4.1. The Amplitude Comparison

As shown in Fig. 7, green dash line and blue line are RCS of the simplified model and the scaled three-blade model in EM simulation, respectively. Red line is RCS result from the simplified model. In this plot, it is clear that the three curves are good matching at major peaks. The mismatch at other positions is thought to result from changes in the shape of the blade and accurate equations in narrow incident angles.

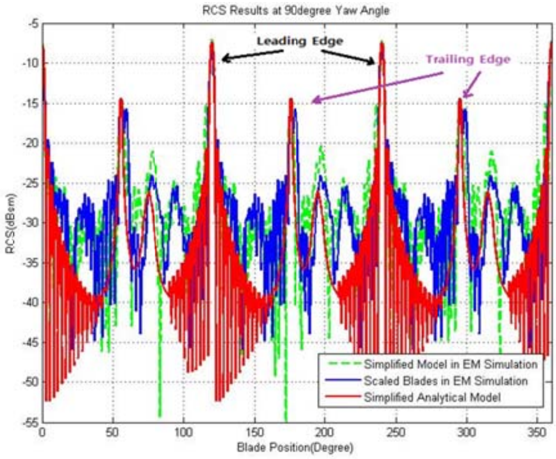

Figure 7: RCS comparison among scaled three-blade (blue line), simplified model (green dash line) in EM simulation and simplified model in mathematical method (red line) when the radar operating frequency is 10.5GHz at 90^o yaw angle.

4.2. The Phase Comparison

Figure 8 presents the phase output comparison between mathematical model (red line) and EM simulation (blue line). It is known that when the blade is perpendicular to the radar LOS, we can get the maximum radial velocity in opposite directions for receding and approaching blades. As expected, phase increases considerably at higher peaks, and decreases at lower peaks. The difference between simple model result and EM simulation output is attributed to the fact that the scaled three-blade model has similar shape as a real turbine blade, whereas the simplified model assumes that the blade is a rectangular plate. This is also the reason that symmetric phase values are generated from the simplified model but the phase curve is asymmetric from EM simulation.

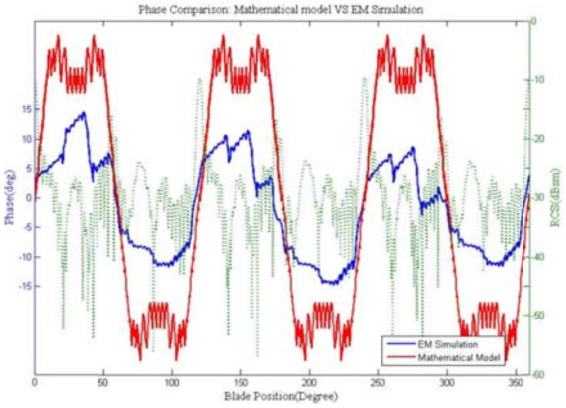

Figure 8: Phase comparison between mathematical model and EM simulation. Red line and blue line is phase signature in mathematical simplified model and EM simulation, respectively. Green dot line is the amplitude in EM simulation.

4.3. The Micro-Doppler Comparison

Figure 9 shows the comparison of Micro-Doppler spectrum between simple analytical model and EM simulation. The total number of flashes observed is six, where each blade has two flashes. The flashes switch up or down in response to the blade edge during rotation: the upper flash is produced by leading edge; the lower flash is result by trailing edge. Despite the fact that Fig. 9 (a) and (b) are largely in agreement, the difference can be noted. The main difference is the power value, because the reflectivity is assumed to be one for analytical calculation.

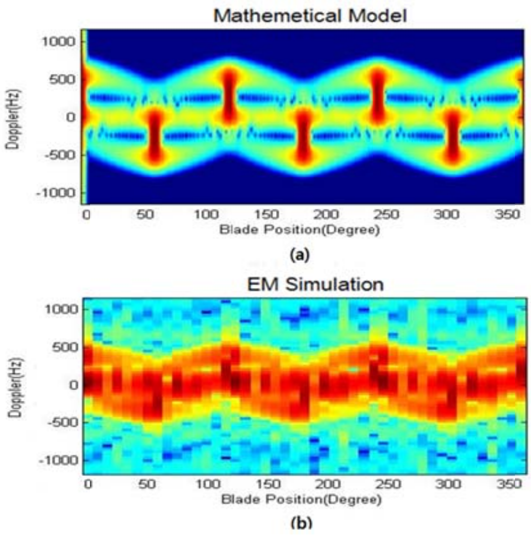

Figure 9: Doppler spectrum signature: (a) produced from mathematical model; (b) produced from EM simulation.

5. SUMMARY

To decrease the computational burden on calculating large size wind turbine models at arbitrary yaw angles, a simplified analytical model is created. The set of simplified analytical model equations can be used for different sizes of turbine structures for all possible blade positions and yaw angles. Although as a tradeoff for simplified geometry and tremendously reduced computational load, outputs from the analytical model cannot perfectly agree with the prediction results from conventional EM solvers, it provides an additional tool for wind turbine recognition and provides the potential solution to alleviate the effect of WTC for weather radar systems.

Continued work is being done to coherently combine amplitude and phase information into a unified model. The future work is to study the effectiveness incorporating of such models in knowledge –aided mitigation and cancellation processing.

6. REFERENCE

1. B. M. Isom, “Characterization and mitigation of wind turbine clutter on the WSR-88D network”.
2. Radar Operation Center, Commerce-Defense-Transportation. Doppler Meteorological Radar WSR-88D. WSR-88D System Specification, May 2007.
3. Chatzigeorgiadis, F., “Development of Code for Physical Optics Radar Cross Section Prediction and Analysis Application”, Master’s Thesis, Naval Postgraduate School Monterey, CA, September 2004.
4. Mahafza, B., Radar Systems Analysis and Design Using MATLAB, London, U.K.: Chapman & Hall/CRC, 2000.
5. Victor C. Chen, The Micro-Doppler Effect in Radar.